

# Tribological response of Powder Metallurgy Magnesium Composite Containing Reactive Amorphous Silica Particles with Porous Structure and Multi-wall Carbon Nanotubes<sup>†</sup>

UMEDA Junko\*, KONDOH Katsuyoshi\*\*, IMAI Hisashi\* and FUGETSU Bunshi\*\*\*

## Abstract

*Powder metallurgy magnesium matrix composite reinforced with un-bundled carbon nanotubes (CNTs) and Mg<sub>2</sub>Si/MgO hybrid compounds were prepared by solid-state synthesis between magnesium powder and amorphous silica particles including CNTs. Their tribological properties were investigated by using the ball-on-disc wear test equipment under dry sliding conditions. The friction coefficient of the composite material was low and stable because of no adhesion and stick-slip phenomenon in contacting with the SUS304 stainless steel ball as a counter material. This was due to both the defensive effect of hard Mg<sub>2</sub>Si dispersoids and the self-lubricant effect of network nanotubes on the sliding surface.*

**KEY WORDS:** (powder metallurgy) (magnesium) (carbon nanotube) (SiO<sub>2</sub>) (Mg<sub>2</sub>Si) (friction coefficient)

## 1. Introduction

From the viewpoint of reducing the energy consumption and improving the mobility of personal digital assistants, magnesium alloys are useful and widely applied to structural components because they are the lightest of the industrial metals in practical use. They are, however, poor in mechanical properties, such as Young's modulus, tensile strength, hardness and heat resistance. In particular, when applying them to friction materials, wear or seizure phenomena easily occur by contacting with the counter materials<sup>1-3)</sup>. Therefore, the additives of hard particles and lubricants are included to improve the mechanical and tribological properties of the conventional magnesium alloys<sup>4-7)</sup>. On the other hand, carbon nanotubes (CNTs), showing excellent characteristics such as high tensile, high elastic modulus, and high hardness, have been considered as useful and attractive additives to organic materials<sup>8,9)</sup>, bulky metals<sup>10,11)</sup> and metallic coatings<sup>12,13)</sup> for tribological and structural applications. In particular, according to theoretical considerations<sup>14)</sup>, the friction coefficient between the walls of multi-walled CNTs should be extremely low. That is, CNT has a significant self-lubricant property and a nano-ball bearing effect<sup>15)</sup>. The bundles of CNTs, are easily formed during the conventional mixing or blending under dry conditions due to van der Waals forces at the most-surface carbon atoms between CNTs, but unfortunately cause the decrease of mechanical and wear properties because the

bundles have poor bonding to the matrix. In order to obtain a stable and low friction coefficient, it is important to control the nanotubes left out from the matrix of the composites during contacting with the counterparts in sliding. On the other hand, magnesium silicides (Mg<sub>2</sub>Si) intermetallics are one of the effective dispersoids to improve the mechanical and tribological performance of magnesium alloys because of their high hardness of 350-700 Hv<sup>16)</sup>. They are easily synthesized by the solid-state reaction of magnesium powder and silicon or silica particles with exothermic heat<sup>17)</sup>. By the synthesis of Mg<sub>2</sub>Si compounds from Mg-SiO<sub>2</sub> elemental mixture powder, magnesium composites reinforced with Mg<sub>2</sub>Si/MgO particles show good wear resistance and anti-offensive performance in sliding wear tests under oil lubricants<sup>18)</sup>. In this study, CNT-SiO<sub>2</sub> composite particles have been employed as the reinforcements for sintered magnesium materials to obstruct the CNTs dropped out from their matrix in sliding. Porous structured SiO<sub>2</sub> particles, originated from rice husks<sup>19)</sup>, were used as raw materials, and dipped into the solutions including un-bundled CNTs. The composite powders were elementally mixed with magnesium powder, and sintered after cold compaction. The microstructural analysis and evaluation of mechanical and tribological behavior of sintered magnesium reinforced with the CNT-SiO<sub>2</sub> composite particles was examined. In particular, the effect of un-bundled CNTs on the wear phenomena and surface damages of the material was investigated by SEM-EDS and XRD analysis.

<sup>†</sup> Received on December 26, 2008

\* Specially Appointed Researcher

\*\* Professor

\*\*\* Professor, Hokkaido University

Transactions of JWRI is published by Joining and Welding Research Institute, Osaka University, Ibaraki, Osaka 567-0047, Japan

## 2. Experimental

### 2.1 Rice husk silica particles

In order to prepare amorphous silica particles with a purity of 99% or more from rice husks, the citric acid ( $C_6H_8O_7$ ) leaching treatment was applied to them at 323 K for 1.8 ks for the removal of metallic impurities such as Ca, K, Na, via the chelate reaction<sup>20)</sup>. After water-rinsing and air drying at 373 K, they were combusted at 1073 K for 3.6 ks under an air supplement of 2.5 ml/s to control the crystallization of silica during burning<sup>21)</sup>. The fragmentation and refinement of the rice husk ashes was carried out by using a ball milling equipment (SEIWA GIKEN, RM-05) for 900 s under a dry condition. Their particle size was measured by a laser diffraction particle size analyzer (HORIBA, Partica LA-920), and their morphology was observed by Field-Emission Scanning Electron Microscope (FE-SEM, JOEL, JSM-6500F) with an Energy Dispersive X-ray spectrometer (EDX). The mean particle size and specific surface area were 12.6  $\mu$  m and 187 m<sup>2</sup>/g, respectively.

### 2.2 CNT-SiO<sub>2</sub> composite particles

Multi-wall carbon nanotubes (MWCNTs, Bayer Material Science), having a diameter of 10 nm and about 1  $\mu$  m length, were used as raw materials. The refined porous silica particles with a large specific surface area of 180~200 m<sup>2</sup>/g<sup>22)</sup> were another raw material and were dipped into the surfactant solution with un-bundled nanotubes, when the CNTs went deep into the silica particles due to their negative zeta potential of -61.8 mV (pH=8.28) in the solution kept at 298 K. With regard to the solutions dispersed with completely split nanotubes, polar zwitterions generally had a high solubility in water, but a poor solubility in most organic solvents. 3-(N, N-dimethylstearylammonio) propanesulfonate, a typical linear zwitterionic surfactant, was used in this study. It had both hydrophobic and hydrophilic groups. Electrostatic interactions, having larger attractive forces than the van der Waals forces between CNTs, occurred at the hydrophilic sites because of the positive charge and negative charges on their headgroups. Therefore, the un-bundled CNTs were dispersed in the zwitterionic surfactant solution<sup>23)</sup>. After dipping and air drying at 353 K, SEM observation was carried out on the silica particles, not only coated with CNTs, but also including them to understand the distribution of nanotubes.

### 2.3 Preparation of sintered magnesium reinforced with CNT-SiO<sub>2</sub> composite particles

The elemental mixture of the above CNT-SiO<sub>2</sub> composite particles and pure magnesium powder, having a mean particle size of 182  $\mu$  m and 98.8 % purity, was prepared as raw material. They were filled into a die with a diameter of 45 mm, and consolidated at room temperature by a 2000 kN hydraulic press machine. Their green compacts with a relative density of 77~79% were sintered at 823 K by spark plasma sintering (SPS, Syntex Inc, SPS-1030) under 30 MPa pressure in vacuum. The

sintered magnesium material including CNT-SiO<sub>2</sub> composite reinforcements was used as a disk specimen for the wear test.

### 2.4 Evaluation

SEM observation of amorphous silica particles with porous structures including CNTs was carried out. Differential Thermal Analysis (DAT, Shimadzu, DTG-60) was conducted on the CNT-SiO<sub>2</sub> composite particles and their elemental mixture with pure magnesium powder from 295 K to 973 K under an argon gas supplement at 2.5 ml/s to evaluate the reaction behavior of the above composite powder and elemental mixtures during heating. XRD analysis and SEM-EDS analysis were carried out to detect the in-situ formed intermetallics of the magnesium composites during sintering. Rockwell type hardness (F-scale, 1/16 inch ball) of the sintered materials was measured by using hardness testing machine (Mitutoyo, ARK-600). The density measure by Archimedes law was applied to the sintered materials. The wear behavior of P/M sintered magnesium composite reinforced with the CNT-SiO<sub>2</sub> composite particles was investigated by using a ball on disk wear test equipment (RHESCA CO LTD., FPR-2100) under air condition. A SUS304 stainless steel ball with 3/4 inch was used as the counter material. The sliding speed was 55 mm/s, and applied load from the SUS304 ball was controlled at 0.5 N. A change in friction coefficient was automatically calculated from the measured friction torque between the SUS304 ball and the magnesium composite disk specimen from PC.

## 3. Results

### 3.1 Reactivity and microstructures

**Figure 1** shows amorphous silica powder, which contains nanotubes in the intra-pores inside, and it consists of the primary ultra-fine silica particles less than 1~2  $\mu$  m. The primary silica reveals a spherical shape, not angular, because they were fractured via a long time ball milling process under a low energy density. The added CNTs are completely de-bundled, and dispersed on the silica particles as shown by the arrows. Furthermore, they exist not only on the surface of silica particles, but also on their inside. **Fig.2** indicates DTA profiles of CNT-SiO<sub>2</sub> composite particles and the elemental mixture of magnesium with the above composite particles (content; 10 mass%) in heating up to 973 K under argon gas supplement 2.5 ml/s. The profile of CNT-SiO<sub>2</sub> composite particles shows no change with exothermic or endothermic heat when heating them up to 973 K. That is, no reaction between nanotubes and SiO<sub>2</sub> amorphous particles occurs, and silicon carbides (SiCs) are not formed in heating less than the melting point of magnesium (923 K). In the case of the elemental mixture of magnesium powder with CNT-SiO<sub>2</sub> composite particles, the exothermically is detected at 720 K, and the exothermic reaction with an extremely large heat occurs at 776 K. The previous study showed the sintering

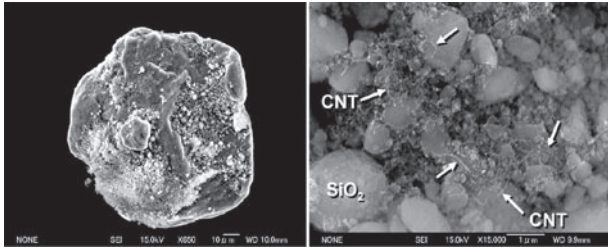


**Fig.1** Granulated amorphous silica particles with porous structure, including un-bundled carbon nanotubes inside (CNT-SiO<sub>2</sub> hybrid particles).

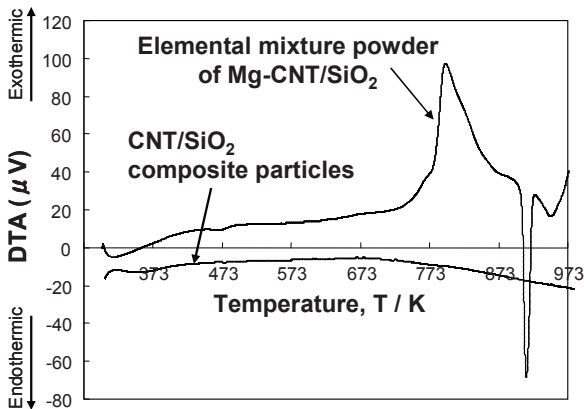
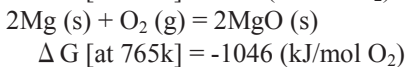
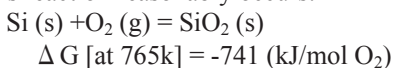


**Fig.2** DTA profiles of CNT-SiO<sub>2</sub> hybrid particles and elemental mixture of magnesium with hybrid particles (content; 10 mass%) in heating up to 973 K under argon gas supplement at 2.5 ml/s.

temperature of 765 K or more was enough to synthesize Mg<sub>2</sub>Si intermetallics from the elemental mixture of magnesium and SiO<sub>2</sub> powders by both deoxidization and oxidation reactions in a solid-state<sup>18)</sup> This is because from a thermodynamic point of view, as shown in below, this reaction reasonably occurs.



Therefore, when heating the CNT-SiO<sub>2</sub> composite particles, the ignition temperature accompanying a large exothermic heat shown in Fig.2 corresponds to the starting temperature to synthesize both Mg<sub>2</sub>Si and MgO hybrid compounds. The structural evaluation by XRD analysis on the sintered magnesium composites consolidated by the SPS process is carried out when applying the sintering temperature of 823 K, which is enough to accelerate the reaction between magnesium and SiO<sub>2</sub> powders as mentioned above. **Figure 3** indicates the XRD patterns of CNT-SiO<sub>2</sub> composite particles (a), sintered pure magnesium (b), sintered magnesium composites including CNT-SiO<sub>2</sub> particles of 5 mass% (c) and 10 mass% (d). In the case of (a), the broad profile with no crystalline peak is detected because of the amorphous silica and with no synthesized compound during sintering. As shown in (b), Mg peaks

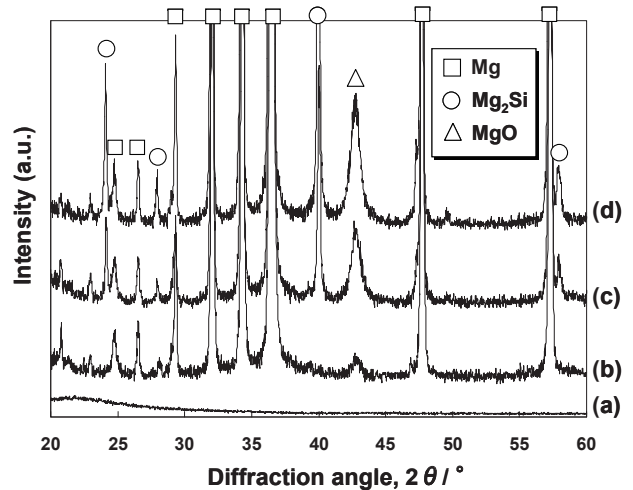


**Fig.3** XRD patterns of CNT-SiO<sub>2</sub> composite particles (a), sintered pure magnesium (b), sintered magnesium composites including CNT-SiO<sub>2</sub> particles of 5 mass% (c) and 10 mass% (d).

are mainly detected in the profile, and a small one of MgO is also observed due to the original surface oxide films of raw magnesium powder. When using the elemental mixture of magnesium and SiO<sub>2</sub> powders, both peaks of Mg<sub>2</sub>Si and MgO are obviously detected in the profile. The intensities of the sintered material containing 10 mass% CNT-SiO<sub>2</sub> composite powders are much larger than those in the case of 5 mass% composite particles. This means that the content of Mg<sub>2</sub>Si and MgO compounds via solid-state synthesis increases during sintering at 823 K. Furthermore, when applying the annealing treatment at 1373 K in argon gas atmosphere to the material (d), no crystalline SiO<sub>2</sub> peak is detected by XRD analysis. In general, the crystallization temperature of the amorphous silica originating from rice husks is 1373 K or more<sup>19)</sup> The fact that the crystalline silica such as cristobalite or tridymite is not observed in the annealed material (d) at 1373 K indicates that the magnesium composite material sintered at 823 K (d) includes no amorphous silica particles, that is, SiO<sub>2</sub> raw particles are completely reacted with magnesium to form both Mg<sub>2</sub>Si and MgO during SPS process at 823 K. **Figure 4** shows SEM-EDS analysis results of sintered magnesium including 10 mass% CNT-SiO<sub>2</sub> hybrid particles (a) and pure magnesium (b). As shown in Fig. 4(a), Si elements are uniformly detected at the primary particle boundaries (PPBs) of the magnesium matrix. This means that the synthesized Mg<sub>2</sub>Si compounds exist at the PPBs, and nanotubes are also dispersed at the same boundaries. On the other hand, pure magnesium sintered material reveals the network-structure MgO at the PPBs shown by arrows in Fig.4 (b). However, it indicates the metallurgical bonding between magnesium powders, without any defects at the boundaries. Table 1 shows Rockwell hardness (scale F) of the sintered magnesium composite including CNT-SiO<sub>2</sub> composite particles as the reinforcements. With an increase in the reinforcement content, the hardness gradually increases, and the composite with 10 mass% composite particles shows

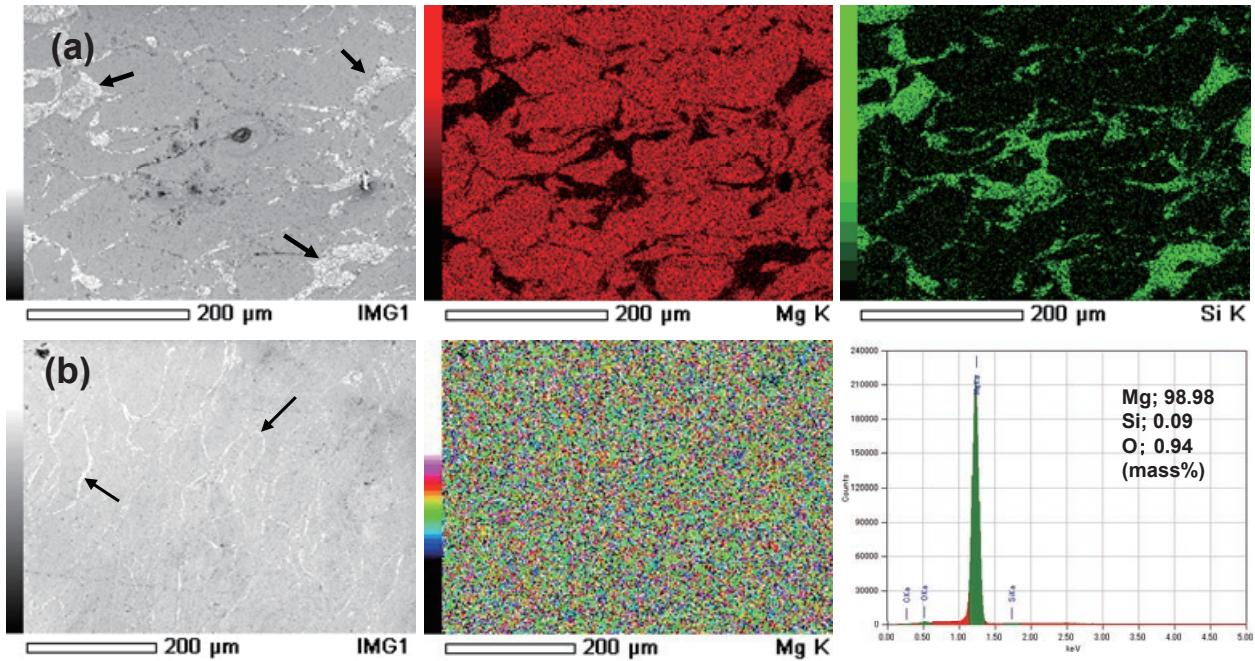


Fig.4 SEM-EDS analysis results of sintered magnesium including 10 mass% CNT-SiO<sub>2</sub> hybrid particles (a) and pure magnesium (b).

twice value as that with no reinforcement. Each sintered material has a relative density of 98% or more, therefore the increase of the hardness is due to the uniform distribution of Mg<sub>2</sub>Si hard compounds<sup>16)</sup> and un-bundled nanotubes in the matrix.

### 3.2 Tribological properties

Figure 5 shows changes of friction coefficient ( $\mu$ ) of sintered magnesium materials including CNT-SiO<sub>2</sub> composite particles of 10 mass% (a), 5 mass% (b) and 0 mass% (c), which are used as the disc specimen, when employing a SUS304 stainless steel ball as the counter material in the dry wear test. In the case of the sintered magnesium reinforced with 10 mass% CNT-SiO<sub>2</sub> composite particles, the friction coefficient is the most stable, and its mean value ( $\mu_0$ ) is lowest of the disc specimens. The  $\mu_0$  value and its instability gradually increases with decreases in the content of the additive composite particles as shown in Fig.5 (b) and (c). The above results mean that the tribological behavior becomes stable through the uniform distribution of the additive reinforcements of sintered magnesium material. Figure 6 reveals the damaged area of the sliding surface of each sintered magnesium disc specimen after the wear test observed by optical microscope. When containing the reinforcement of 10 mass% CNT-SiO<sub>2</sub> composite particles (a), a slightly abrasive wear, but no adhesion is observed on the sliding surface. The black area corresponds to Mg<sub>2</sub>Si compounds and CNTs as shown in (a-1). This represents a smooth sliding condition between the magnesium composite and SUS304 ball under dry conditions. In the case of (b), the main damages are due to the severely abrasive wear in contact with the counter material, but some adhesives and plastic deformation are also detected. When no reinforcement is included in the

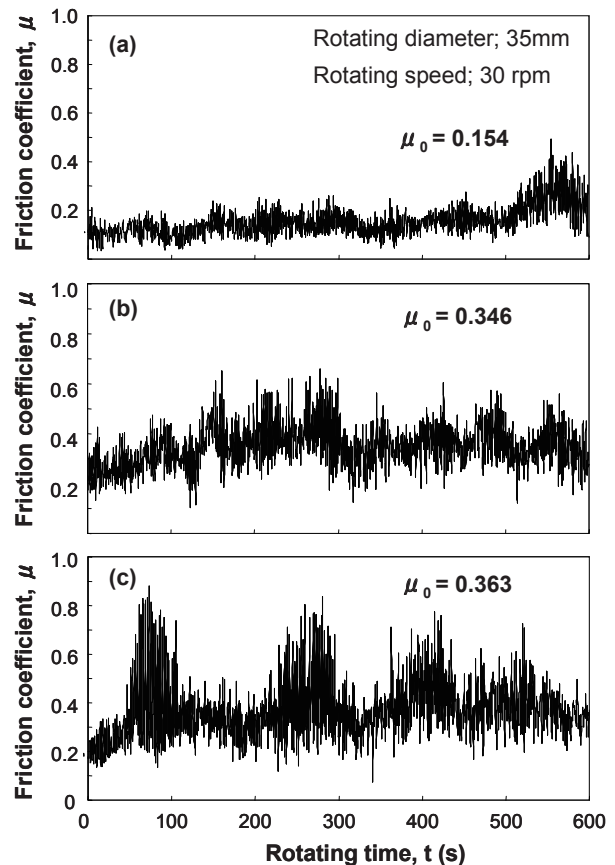
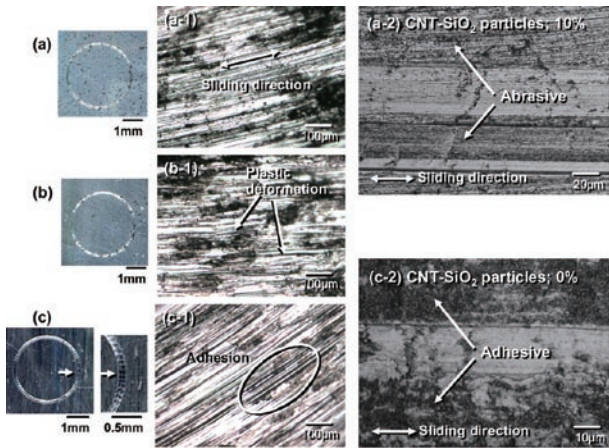


Fig.5 Changes of the friction coefficient ( $\mu$ ) of sintered magnesium materials including CNT-SiO<sub>2</sub> composite particles of 10 mass% (a), 5 mass% (b) and 0 mass% (c), which are used as disc specimen, when employing a SUS304 stainless steel ball as counter material in the dry wear test.



**Fig.6** Damaged area of sliding surface of each sintered magnesium disc specimen after wear test observed by optical microscope: CNT-SiO<sub>2</sub> composite particles of 10 mass% (a), 5 mass% (b) and 0 mass% (c).

sintered material (c), both severely abrasive wear in (c-1) and adhesion phenomena corresponding to the dark areas shown in (c-2) are clearly observed at the sliding surface. The macro-observation on the surface shown in (c) also indicates the stripe pattern damages vertical to the sliding direction. This is caused by a “stick-slip” phenomenon due to the periodic repetition of the adhesion and detachment of the metals on the counter material under the dry sliding condition<sup>24)</sup> As a result, a friction coefficient profile shown in Fig.5 (c) indicates a typical behavior with a sharp fluctuation corresponding to a “stick-slip” phenomenon.

**Figure 7** indicates the SEM-EDS analysis result on the PPB, where the synthesized Mg<sub>2</sub>Si and MgO compounds exist, on the sliding surface of the sintered magnesium composite with the reinforcement of 10 mass% after wear test. In the magnified area of the reinforcement of Fig.7 (b), it consists of the white particles, corresponding to Mg<sub>2</sub>Si and MgO hybrid compounds, and un-bundled nanotubes. There is no detached Mg<sub>2</sub>Si and MgO compound from the sliding surface because of a strong bonding between the magnesium matrix and their compounds via solid-state synthesis. In particular, the

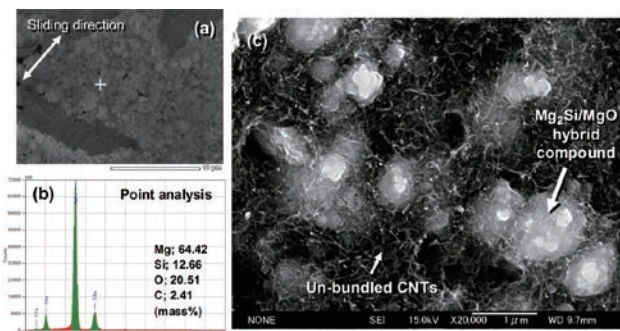


**Fig.7** SEM-EDS analysis result on primary particle boundaries, where synthesized Mg<sub>2</sub>Si and MgO compounds exist, on sliding surface of sintered magnesium composite with reinforcement of 10 mass% after wear test.

network CNTs are formed around the synthesized composite particles and the individual CNT covers the sliding surface. Accordingly, the reason why the sintered magnesium composite with CNT-SiO<sub>2</sub> composite particles showed a superior tribological behavior with a low and stable friction coefficient is due to both improved defenses by the synthesized Mg<sub>2</sub>Si hard particles<sup>17)</sup> and self-lubricant and bearing effect of the network of un-bundled nanotubes dispersed in the matrix.

#### 4. Conclusion

The sintered magnesium composite material reinforced with the carbon nanotubes and Mg<sub>2</sub>Si/MgO hybrid particles has been developed by a powder metallurgy process when using the elemental mixture of pure magnesium and amorphous porous silica containing CNTs inside as a starting material. During sintering the mixture powder, the solid-state synthesis of Mg<sub>2</sub>Si and MgO via deoxidization and oxidation reaction occurred. The tribological properties of the sintered magnesium material were significantly improved by the additive reinforcement, and the friction coefficient was low and stable under the dry sliding condition. Hard Mg<sub>2</sub>Si intermetallic were effective for the wear resistance in contacting a SUS304 stainless steel ball, and nanotubes had an important role to form the lubricant condition at the interface between the sintered magnesium and the counter material due to their network structure on the sliding surface.

#### Acknowledgement

The authors acknowledge the financial support of Hosokawa Powder Technology Foundation.

#### References

- 1) Weijiu Huang, Bin Hou, Youxia Pang, Zhongrong Zhou, *Wear*, 260 (2006) 1173-1178.
- 2) J. An, R.G. Li, Y. Lu, C.M. Chen, Y. Xu, X. Chen, L.M. Wang, *Wear*, 265, (2008) 97-104.
- 3) Naing Naing Aung, Wei Zhou, Lennie E.N. Lim, *Wear*, 265 (2008) 780-786.
- 4) C.Y.H. Lim, D.K. Leo, J.J.S. Ang, M. Gupta, *Wear*, 259 (2005) 620-625.
- 5) S. C. Sharma, B. Anand, M. Krishna, *Wear*, 241 (2000) 33-40.
- 6) Q.B. Nguyen, M. Gupta, *Composites Science and Technology*, 68 (2008) 2185-2192.
- 7) X.J. Wang, X.S. Hu, K. Wu, K.K. Deng, W.M. Gan, C.Y. Wang, M.Y. Zheng, *Materials Science and Engineering: A*, 492, (2008) 481-485.
- 8) X.H. Men, Z.Z. Zhang, H.J. Song, K. Wang, W. Jiang, *Composites Science and Technology*, 68 (2008) 1042-1049.
- 9) L.C. Zhang, I. Zarudi, K.Q. Xiao, *Wear*, 261 (2006) 806-811.
- 10) S.M. Zhou, X.B. Zhang, Z.P. Ding, C.Y. Min, G.L. Xu, W.M. Zhu, *Composites: Part A*, 38 (2007) 301-306.
- 11) K.T. Kim, S.I. Cha, S.H. Hong, *Materials Science and*

## Tribological Response of Powder Metallurgy Magnesium Composite Containing Reactive Amorphous Silica Particles

- Engineering A, 449–451 (2007) 46–50.
- 12) W.X. Chena, J.P. Tub, L.Y. Wangb, H.Y. Gana, Z.D. Xua, X.B. Zhangb, Carbon, 41 (2003) 215–222.
  - 13) L.Y. Wang, J.P. Tu, W.X. Chen, Y.C. Wang, X.K. Liu, Charls Olk, D.H. Chengd, X.B. Zhang, Wear, 254 (2003) 1289-1293.
  - 14) M. Damnjanovic, T. Vukovic, I. Milosevic, European Journal of Physics B, 25 (2002) 131-134.
  - 15) H.W. Kroto, J.R. Heath, S.C. O'Brien, R.F. Curl, R.E. Smalley, Nature 318 (1985) 162-3.
  - 16) L. F. Mondolfo, Aluminum Alloys: Structure and Properties, Butterworths, London (1976) 566.
  - 17) K. Kondoh, H. Oginuma, A. Kimura, S. Matsukawa, and T. Aizawa, Materials Transactions, 44 (2003) 981-985.
  - 18) K. Kondoh, H. Oginuma, and T. Aizawa, Materials Transactions, 44 (2003) 524-530.
  - 19) J. Umeda, K. Kondoh, Y. Michiura, Materials Transactions, 48 (2007) 3095-3100.
  - 20) J. Umeda, K. Kondoh, Y. Michiura, Transactions of Joining and Welding Research Institute, 36 (2007) 17-21.
  - 21) K. Kondoh, H. Oginuma, J. Umeda, T. Umeda, Materials Transactions, 46 (2005) 2586-2591.
  - 22) M.F. de Souza, P.S. Batista, I. Regiani, J.B.L.Liborio, D.P.F. de Souza, Materials Research, 3 (2000) 25-30.
  - 23) B. Fugetsu, W. Han, N. Endo, Y. Kamiya, T. Okuhara, Chemistry Letter, 34 (2005) 1218-1219.
  - 24) R. Smith, D. Mulliah, S.D. Kenny, E. McGee, A. Richter, M. Gruner, Wear, 259 (200) 459-466.